Monitoring Daily Dynamics of Early Tumor Response to Targeted Therapy by Detecting Circulating Tumor DNA in Urine

Hatim Husain[1], **Vladislava O. Melnikova**[2], **Karena Kosco**[2], **Brian Woodward**[1], **Soham More**[1], **Sandeep C. Pingle**[2], **Elizabeth Weihe**[1], **Ben Ho Park**[3], **Muneesh Tewari**[4], **Mark G. Erlander**[2], **Ezra Cohen**[1], **Scott M. Lippman**[1], and **Razelle Kurzrock**[1]

[1]University of California San Diego, Moores Cancer Center, La Jolla, CA USA

[2]Trovagene Inc., San Diego, CA USA

[3]Johns Hopkins Sidney Kimmel Cancer, Baltimore MD USA

[4]University of Michigan, Ann Arbor, MI USA

Abstract

Purpose—Non-invasive drug biomarkers for the early assessment of tumor response can enable adaptive therapeutic decision-making and proof-of-concept studies for investigational drugs. Circulating tumor DNA (ctDNA) is released into the circulation by tumor cell turnover and has been shown to be detectable in urine.

Experimental Design—We tested the hypothesis that dynamic changes in epidermal growth factor receptor (EGFR) activating (exon 19del and L858R) and resistance (T790M) mutation levels detected in urine could inform tumor response within days of therapy for advanced non-small cell lung cancer (NSCLC) patients receiving osimertinib, a second line third generation anti-EGFR tyrosine kinase inhibitor.

Results—Eight of nine evaluable NSCLC patients had detectable T790M-mutant DNA fragments in pre-treatment baseline samples. Daily monitoring of mutations in urine indicated a pattern of intermittent spikes throughout week 1 suggesting apoptosis with an overall decrease in fragment numbers between baselines to day 7 preceding radiographic response assessed at 6-12 weeks.

Conclusions—These findings suggest drug-induced tumor apoptosis within days of initial dosing. Daily sampling of ctDNA may enable early assessment of patient response and proof-of-concept studies for drug development.

Keywords

Circulating tumor DNA (ctDNA); urine; epidermal growth factor (EGFR); non-small cell lung cancer (NSCLC); osimertinib

---

Corresponding author: Hatim Husain MD, UCSD Moores Cancer Center, 3855 Health Sciences Dr #0987, La Jolla, CA 92093, hhusain@ucsd.edu.

Introduction

Non-invasive drug biomarkers for the early assessment of tumor response has impacted therapeutic decision-making for the multiple targeted therapy options currently available for cancer treatment (1). Morphological or functional assessment of tumor burden using computed tomography (CT), magnetic resonance imaging (MRI), or positron emission tomography (PET) remains the standard of care for response assessment. However, conventional imaging lacks fundamental information regarding the tumor DNA mutation status, tumoral heterogeneity, and intrinsic tumor biology. Furthermore, conventional imaging modalities can be subject to confounding variables that mimic tumor progression or response depending on the tumor type (i.e., pseudo-progression or pseudo-response) (2). Strategies to characterize the molecular evolution of a tumor through repeat tissue biopsies are being used for therapeutic decision-making and/or pharmacodynamic evaluation of investigational drugs in lung cancer management but are increasingly becoming a less viable option given the invasiveness of the procedure, potential complications associated with tissue biopsy procedures, practical concerns around the scheduling and frequency of testing, and an inherent inability to characterize intra-and inter-lesional heterogeneity in a single lesion tissue biopsy (3).

Circulating tumor DNA (ctDNA) is released into the circulation from tumor cells with greater quantities present as tumor volume and cellular turnover increase (3-4). ctDNA is highly degraded (~166bp) with classic apoptotic DNA size laddering defined by histone size and is most likely derived from apoptotic turnover of tumor cells (4). The proportion of ctDNA to total cell-free wild-type DNA present in blood varies widely from very rare (0.01%) to highly prevalent (>90%) and is histology and tumor-burden dependent (3-6). ctDNA biomarkers in blood can be concordant with patient-matched tissue biopsies, can identify intra- and inter-lesional heterogeneity, and can correlate with responsiveness to therapy (5-14). ctDNA present in blood can be excreted into urine, and patient-matched tissue, plasma and urine studies indicate concordance of DNA mutation status and suggest comparable sensitivities across the three biospecimens (15-18). Urine sampling provides a non-invasive source of ctDNA from cancer patients and daily urine collection can be facilitated.

We hypothesized that one may detect kinetic changes in the amount of DNA released within days after drug administration. We tested this hypothesis by monitoring the daily tumor dynamics of epidermal growth factor receptor (*EGFR*) activating mutations (L858R, exon 19 deletions) and resistant mutation (T790M) in urine from patients with metastatic non-small cell lung cancer (NSCLC) receiving the third generation tyrosine kinase inhibitor osimertinib. Third generation anti-*EGFR* tyrosine kinase inhibitors (TKIs) are highly active against *EGFR* T790M-bearing NSCLC with agents approved by the US Food and Drug Administration or in various stages of clinical development (osimertinib, rocelitinib, HM61713, ASP827, EGF816, and PF7775) (19-23). Osimertinib received accelerated approval by the US FDA in November 2015 (23), and the clinical benefit rate of the compound (complete response, partial response, and stable disease by RECIST 1.1) was 93% in a phase III study with a significant improvement in progression free survival compared to chemotherapy (10.1mos vs 4.4mos, p=0.001) (24).

METHODS

Patients

Ten subjects with *EGFR* mutant NSCLC undergoing treatment with erlotinib or afatinib were included in the study, and nine subjects had evaluable serially collected samples. Two patients with daily collections not on therapy were analyzed as controls. On progression, tissue biopsies were performed, and if positive for T790M, patients were started on osimertinib 80mg orally daily. Those patients who had serial collections prior to second line therapy had samples interrogated. Between 60-120 mL of urine were collected at each time point. Urine samples were de-identified for the staff performing ctDNA testing, and operators performing urine ctDNA analyses were blinded to the radiographic changes pertinent to each patient. For early response monitoring, urine samples were collected before drug initiation on day 0 (baseline), daily at a consistent time before drug during the first week of osimertinib, and then approximately every 3 weeks until progression. All evaluable patients had daily urine collections during a first morning void before drug consumption. The study was conducted in accordance with recognized ethical guidelines and written informed consent obtained in accordance with UCSD IRB guidelines.

Analysis of tissue biopsies

Molecular analysis of formalin-fixed paraffin-embedded (FFPE) tumor tissue biopsies was performed within 28 days of radiologic progression on first-line anti-*EGFR* TKI using the Cobas® *EGFR* Mutation Test (Roche Molecular Systems).

Radiographic assessments

The overall response rate was assessed according to investigator review with Response Evaluation Criteria in Solid Tumors v1.1 (RECIST) analyses performed by a dedicated lung cancer radiologist at the University of California San Diego. Patients were assessed at baseline with CT/MRI scans approximately every 6 weeks from the time of first dose.

ctDNA *EGFR* mutational analysis

Urinary ctDNA extraction—Urine was collected in 120 mL collection vessels; proprietary preservative was added immediately after urine collection. Urine was concentrated to 4ml using a Vivacell 100 (Sartorius Corp, Bohemia, NY) and incubated with 700 uL of Q-sepharose Fast Flow quaternary ammonium resin (GE Healthcare, Pittsburg, PA) and 20 mL binding buffer. Following incubation at room temperature for 1 hour, tubes were spun to collect sepharose and bound DNA. The pellet was resuspended in a buffer containing guanidinium hydrochloride and isopropanol, and the eluted DNA was collected as a flow-through using polypropylene chromatography columns (BioRad Laboratories, Irvine, CA). The eluate was further purified using QiaQuick columns (Qiagen, Germany).

Quantitative ctDNA analysis—Extracted DNA was quantitated using a droplet digital PCR (ddPCR) assay that amplifies a single copy RNaseP reference gene (QX200 ddPCR system, Bio-Rad, CA). Quantitative analysis of *EGFR* activating mutations and T790M resistance mutation was performed using mutation enrichment PCR coupled with next-generation sequencing detection (MiSeq, Illumina Inc., CA). Mutation enrichment was

accomplished via short amplicon (42-44 base pairs), kinetically driven enrichment PCR that selectively amplifies mutant fragments while suppressing amplification of the wild-type sequence using blocker oligonucleotide. The following primers were used for PCR amplification: T790M, forward, CS1-TGGTTCTACACTCCACCGTGCARCTCATC, reverse, CS2-GGCAGCCGAAGGGCAT; Exon19 deletions, forward: CS1-AATTCCCGTCGCTATC, reverse: CS2-TTCCTTGTTGGCTTTCG; L858R, forward: CS1-GCATGTCAAGATCACAG, reverse: CS2-CGCACCCAGCAGTTTG. PCR enrichment cycling conditions utilized the initial 98°C denaturation step followed by the assay-specific 5 to 15 cycles of pre-amplification PCR and 17 to 32 cycles of mutation enrichment PCR. Following enrichment PCR, custom DNA libraries were constructed and indexed using Access Array System for Illumina Sequencing Systems (Fluidigm Corp, San Francisco, CA). The indexed libraries were pooled, diluted to equimolar amounts with buffer and the 5% PhiX Control library, and sequenced to 200,000x coverage on an Illumina MiSeq platform using 150-V3 sequencing kits (Illumina, Inc. CA). Primary image analysis, secondary base-calling and data quality assessment were performed on the MiSeq instrument using RTA v1.18.54, and MiSeq Reporter v2.6.2.3 software (Illumina Inc., CA). Analysis output files (FASTQ) from the run were processed using a custom sequencing reads counting and variant calling algorithm to tally the sums of total target gene reads, wild-type or mutant *EGFR* reads that passed sequence quality criteria (qscore 20). A custom quantification algorithm was developed to accurately determine the absolute number of mutant DNA molecules in the source ctDNA sample. Each single multiplexed MiSeq NGS run contained, in addition to clinical samples and controls, 12 standard curve samples (3 replicates with known mutant input copies at 4 levels). Cell line DNA and short, ~200bp double-stranded oligonucleotides (gBlocks Gene Fragments, IDT, Coralville, IA) were used to generate reference standards and controls. Mutant reads in a test sample were converted to absolute mutant copy number in the original sample by interpolation to the standard curve. In order to account for biological variability of DNA concentration in urine, the number of mutant copies detected was standardized by normalizing the number of copies detected in the sample to a constant number of calculated genome equivalents of wild-type DNA across all samples to yield concentration of mutant fragments (i.e., 60 ng wild-type DNA = 18,180 genome equivalents [GEq]; 330 ng wild-type DNA = 100,000 GEq). Testing of analytical performance of the *EGFR* mutation detection assays demonstrated that absolute measurements by mutation enrichment NGS across three *EGFR* assays corresponded to 107% ± 40.2% of input mutant copies, with mean Coefficient of Variation Percent (CV%) of 34.5% across 5-250 input mutant copy range, indicating efficiency in absolute detection by enrichment PCR-NGS (Supplementary Figure 1).

When quantifying rare DNA fragments, the frequency distribution of the number of DNA molecules that are present for measurement in each PCR tube were predicted by Poisson distribution. If a PCR reaction is expected to contain a single molecule of target DNA, Poisson distribution predicts probabilities of 36.8, 18.4, and 6.1% for 0, 1, 2, and 3 molecules, respectively, to be present in the PCR tube. The lower level of detection (LLoD) was defined as the lowest number of copies for which the frequency distribution of the copy number events upon repeated measurements fell within the 95% confidence interval of expected frequency distribution determined by Poisson statistics. For LLoD finding and

verification, 80 repeated measurements were performed on a single multiplexed NGS run for each spike-in level of 1, 2 or 3 mutant *EGFR* copies within 18,181 genome equivalents (60 ng) of *EGFR* wild-type DNA. The observed frequency distribution for mutant copy events was compared to the expected frequency. For sample preparation, stock DNA solutions of 100 mutant copies per μL were prepared using cell line DNA quantified using ddPCR (RainDance, Billerica, MA), and then diluted serially to a target copy level in 18,181 GEq of *EGFR* wild-type DNA. The number of mutant *EGFR* copies in each measured dilution sample was determined by interpolating the number of NGS reads to a standard curve. Lower Limit of Blank (LLoB) was calculated for each *EGFR* assay using samples containing *EGFR* wild-type DNA.

Clinical *EGFR* mutation detection cut-offs

Clinical *EGFR* mutation detection cut-offs were determined by analyzing 200 urine DNA samples obtained from unique healthy volunteers and metastatic patients with non-EGFR mutant, non-NSCLC malignancies. Mutation-specific cut-offs were set to the median plus three standard deviations of the mutant *EGFR* copy counts in the urine samples from an *EGFR* mutation-negative population. Detection cut-offs were standardized to 100,000 wild-type genome equivalents (GEq) yielding adjusted clinical detection cut-offs of 5.5, 5.5 and 12.6 for exon 19 deletions, L858R and T790M, respectively.

A. Statistical Analysis

Analysis of trends observed in urine ctDNA *EGFR* signal at one to two weeks upon patient treatment with osimertinib was assessed using Wilcoxon's paired two-sample test with a one-sided p-value. P values less than 0.05 were considered statistically significant. Correlation between input and output absolute *EGFR* mutant copies in the analytical spike-in experiments was examined using Spearman's correlation, which allows one to account for the non-linearity of variables. Analytical variability of the assays was examined using the Coefficient of Variation Percent (CV%), calculated as the ratio of the standard deviation to the mean of the absolute *EGFR* copies detected within each absolute copy per input level and is reported as a percentage. All statistical analyses were carried out using R v3.2.3 computer software.

Results

Detection of ctDNA mutant *EGFR* DNA fragments in urine

To overcome the inherent technical challenges of detecting degraded ctDNA having rare prevalence within cell-free wild-type DNA, assays for the detection of *EGFR*-activating mutations (exon 19 deletions, L858R) and resistance mutation T790M were developed to generate short amplicon lengths of 33bp, 46bp and 44bp, respectively. Subsequent polymerase chain reaction (PCR) amplification using wild-type blockers was done to enrich for mutant ctDNA, and quantitation of mutant sequences was achieved by next generation sequencing. Using this approach, the analytical lower limit of detection of the exon 19 deletions, L858R and T790M assays was 1, 1 and 2 copies respectively in a background of approximately 18,180 wild-type genome equivalents or a mutant fraction range of 0.006-0.010% (18). (Table 1) To account for biological variability of urine sampling, copies

reported herein are standardized to 100,000 wild-type genome equivalents (GEq) yielding an adjusted lower limit of detection of 5.5, 5.5 and 11 for exon 19 deletions, L858R and T790M, respectively. Concurrent standard curves were assayed with patient samples for accurate determination of the absolute number of mutant DNA molecules in each urine sample.

Ten patients with locally advanced or metastatic NSCLC and radiologically documented progression from treatment with erlotinib or afatinib had samples evaluated; only nine had available daily serial urine samples including a sample at baseline. All nine patients had a positive tissue biopsy for the *EGFR*-activating mutations (exon 19 deletion, L858R, and L861Q) and the resistance mutation T790M (Table 2). Detectable T790M mutant DNA fragments were observed in baseline urine samples in 8 out of 9 patients (median = 70 copies; range 18 to 2,684) with concordant *EGFR*-activating mutation (L858R, exon 19 deletions) DNA fragments in 7 of 8 patients (median = 167 copies; range 10 to 9,745); one patient had a tissue biopsy *EGFR* exon 21 L861Q mutation that was not assayed in urine (Table 2, Patient 10). Overall, the percent of mutant *EGFR* fragments versus wild-type DNA ranged over 100-fold from 0.033% to 12.4% in urine DNA.

Monitoring early tumor response to third generation tyrosine kinase inhibitors in urine

To quantitate and trend the dynamics of the *EGFR* mutational load in urine of patients treated with osimertinib, ctDNA was assessed at baseline, followed by collection of daily samples for seven days and then approximately every 3 weeks. Two evaluable patients had several months of longitudinal samples prior to second line of therapy. After the administration of drug, a significant peak in the amount of ctDNA detected in the urine was observed within days of initiation of second line therapy (Figure 1). Peaks were observed among the patients who had longitudinal samples collected before the second line therapy was initiated.

Eight patients who received second line therapy with osimertinib achieved clinical benefit, as evidenced by the radiographic assessment at 6 and 12 weeks after therapy: seven patients had response after treatment with greater than thirty percent reduction in target lesions and one patient (subject 41) had stable disease for six months by RECIST 1.1 measurements (Table 2).

All 8 patients with detectable *EGFR* T790M baselines had the presence of spikes within the first week of therapy and then a large decrease in the number and percent of copies detected from baseline compared to week 1 and 2 for *EGFR* T790M and the activating mutations L858R and exon 19 deletion (Figure 2, 3). The peaks in detectable T790M were identified before the decrease from baseline to week 1 (median 66.5% decrease, p=0.014) and week 2 (median 100% decrease, p=0.045). Peaks in ctDNA for the *EGFR* activating L858R and exon 19 deletions were observed followed by a decreasing trend with a median 86% and 81% decrease in signal at weeks 1 and 2, respectively for L858R and exon 19 deletions (Figure 3). In subjects 1, 20, 22, and 41, the spike in mutant ctDNA was followed by a decrease as early as day 4. Matching kinetics of early response was observed for the corresponding *EGFR*-activating mutations L858R and exon 19 deletions with overall numbers of copies mostly higher than for T790M. Following these early temporal spikes,

low steady-state levels of ctDNA *EGFR* appeared to be established after 1 to 2 weeks on treatment and persisted for many months (Figure 2). In subject 22, the low steady state levels persisted to 129 days while the patient was on therapy. The temporal spikes and the subsequent rapid loss of mutant *EGFR* ctDNA in urine after the first 1 to 2 weeks of treatment were associated with and preceded the assessment of radiographic response, as measured 6 and 12 weeks following the initiation of therapy.

CT scan best responses by RECIST 1.1 are noted in Table 2. Subjects 16 and 22 had the most significant percentage reduction in tumor volume by RECIST measurements and had the highest baseline quantity of *EGFR* T790M detected. Patients with stage M1b (extra-thoracic metastasis) NSCLC had higher baseline *EGFR* mutant copies identified compared with subjects with M1a disease (intra-thoracic metastasis). For all daily samples, urine volumes, DNA concentrations, DNA input amounts, the number of output mutant sequencing reads, mutant copies detected and the 95% Confidence Intervals are shown in Supplemental Table 1. In two patients who had daily collections not on therapy, there were no peaks identified during daily collection.

Discussion

Daily monitoring of ctDNA by non-invasive sampling of patients receiving oncogene defined targeted therapy can enable temporal and quantitative dissection of early tumor response. Both the patient-dependent intermittent peaks of levels for *EGFR*-activating mutations L858R, exon 19 deletions, and resistant mutation T790M and the rapid overall decrease in the number of copies during the first week indicate that second-line third generation anti-*EGFR* TKI treatment induces tumor cell apoptosis within days of drug administration. Temporal spikes in ctDNA were unlikely to be generated by assay variability as no peaks were identified for patients with daily collection not on therapy, and the mutation copies at peak levels were significantly different from pre-treatment or adjacent time points based on the empirically derived 95% Confidence Intervals (Figure 1, Supplemental Table 1) as well as assay CV% (Supplemental Figure 1). Pre-treatment time points show a significantly different profile as compared to post-treatment samples with an immediate quantitative rise in the number of *EGFR* copies after therapy reflecting cell apoptosis within days of exposure to drug (Figure 1). Pre-clinical studies of third generation anti-*EGFR* tyrosine kinase inhibitors in tumor xenograft mouse models demonstrated a strong inhibition of both phospho-*EGFR* and downstream signaling pathways with significant tumor shrinkage at days 5 to 7 from dose initiation (25-27). Third generation anti-*EGFR* inhibitors are known to cause apoptosis in pre-clinical models, and the combination of Bcl-2 and Bcl-XL inhibitors with third generation inhibitors induced more apoptosis demonstrating the importance of apoptotic pathways in cytoreduction on third generation TKI therapy (28).

Kinetic daily ctDNA monitoring may have the potential utility to act as an early pharmacodynamic biomarker for proof-of-concept studies of targeted therapies in development. This approach may be explored to determine whether an investigational drug induces apoptosis of the targeted tumor cells (i.e., drug target inhibition) by quantitating the daily changes in ctDNA levels of the targeted tumor DNA mutation(s). The clinical benefit

rate of osimertinib in EGFR T790M positive patients is extremely high (93%) with only 6% of patients progressing after initial scans (24), and in our cohort we did not have patients who progressed on initial scans after osimertinib initiation. Further work will characterize response assessments in patients prospectively based on the size, presence, or absence of peaks identified (Figure 4). For chemotherapies and immunotherapies that do not target a specific tumor genomic alteration, further studies will explore the possibility of quantitating total levels of tumor DNA mutation(s) prevalent for the tumor type under investigation. The identification of kinetic changes in ctDNA during early time-points may provide a practical opportunity to intervene earlier with combinatorial strategies that anticipate specific resistance mechanisms.

In this pilot study, we observed the novel finding of ctDNA spikes within one to two weeks of therapy, and in some patients as early as day 4. A subsequent decrease relative to baseline for both the *EGFR*-activating mutations L858R and exon 19 deletions and the resistance mutation T790M was seen. This pattern during the first week was associated with subsequent clinical benefit for all eight patients (7 with partial response, 1 with stable disease) by RECIST radiographic assessment at 6 and 12 weeks after therapy initiation. Two patients who had the most significant percent reduction in tumor burden on CT scans also had the highest detectable quantity of EGFR T790M in baseline samples. Patients with M1a disease had lower EGFR T790M detection compared to patients with M1b disease suggesting extra-thoracic metastasis is more predictive of ctDNA detection. Our study is the first significant attempt to our knowledge to describe the kinetic rise in the number of copies of ctDNA immediately after therapy, and our findings are consistent with previously reported studies in plasma demonstrating an overall decrease in ctDNA levels for patients responding to targeted therapy with samples collected weeks to months after initiation of therapy (13, 29-30). Studies are ongoing to further understand the impact of biological factors including urine volume and residency time, timing of collection, locus dependent pattern of ctDNA degradation, and patients' hydration status on the dynamics and detection of ctDNA in urine.

A desirable capacity in cancer therapeutic decision-making is to have the ability to make an early assessment of patient responsiveness to therapy, and daily kinetic monitoring of ctDNA may facilitate a refined paradigm in individualized patient care. Faster assessment of patient response can aid in navigating adaptive therapy strategies to reduce drug toxicity, identify resistance to therapy, and enable consideration of alternate, potentially more efficacious therapies. Further prospective studies will evaluate larger cohorts of patients to understand how the size, presence, and absence of peaks correlate with response assessments and how quantitative and qualitative evaluation of specific clonal populations that persist after initial cytoreduction may be relevant for characterizing minimal residual disease.

Supplementary Material

Refer to Web version on PubMed Central for supplementary material.

References

1. Gainor JF, Longo DL, Chabner BA. Pharmacodynamic biomarkers: falling short of the mark? Clin Cancer Res. 2014; 20:2587–2594. [PubMed: 24831281]

2. Kurzrock R, Atkins J, Wheler J, Fu S, Naing A, Busaidy N, et al. Tumor marker and measurement fluctuations may not reflect treatment efficacy in patients with medullary thyroid carcinoma on long-term RET inhibitor therapy. Ann Oncol. 2013; 24:2256–2261. [PubMed: 23676418]

3. Diaz LA Jr, Bardelli A. Liquid biopsies: genotyping circulating tumor DNA. J Clin Oncol. 2014; 32:579–586. [PubMed: 24449238]

4. Jahr S, Hentze H, Englisch S, Hardt D, Fackelmayer FO, Hesch RD, et al. DNA fragments in the blood plasma of cancer patients: quantitations and evidence for their origin from apoptotic and necrotic cells. Cancer Res. 2001; 61:1659–1665. [PubMed: 11245480]

5. Haber DA, Velculescu VE. Blood-based analyses of cancer: circulating tumor cells and circulating tumor DNA. Cancer Discov. 2014; 4:650–661. [PubMed: 24801577]

6. Bettegowda C, Sausen M, Leary RJ, Kinde I, Wang Y, Agrawal N, et al. Detection of circulating tumor DNA in early- and late-stage human malignancies. Sci Transl Med. 2014; 6:224ra224.

7. Diaz LA Jr, Williams RT, Wu J, Kinde I, Hecht JR, Berlin J, et al. The molecular evolution of acquired resistance to targeted EGFR blockade in colorectal cancers. Nature. 2012; 486:537–540. [PubMed: 22722843]

8. Leary RJ, Sausen M, Kinde I, Papadopoulos N, Carpten JD, Craig D, et al. Detection of chromosomal alterations in the circulation of cancer patients with whole-genome sequencing. Sci Transl Med. 2012; 4:162ra154.

9. Piotrowska Z, Niederst MJ, Karlovich CA, Wakelee HA, Neal JW, Mino-Kenudson M, et al. Heterogeneity Underlies the Emergence of EGFRT790 Wild-Type Clones Following Treatment of T790M-Positive Cancers with a Third-Generation EGFR Inhibitor. Cancer Discov. 2015; 5:713–722. [PubMed: 25934077]

10. Janku F, Vibat CR, Kosco K, Holley VR, Cabrilo G, Meric-Bernstam F, et al. BRAF V600E mutations in urine and plasma cell-free DNA from patients with Erdheim-Chester disease. Oncotarget. 2014; 5:3607–3610. [PubMed: 25003820]

11. Karachaliou N, Mayo-de las Casas C, Queralt C, de Aguirre I, Melloni B, Cardenal F, et al. Association of EGFR L858R Mutation in Circulating Free DNA With Survival in the EURTAC Trial. JAMA Oncol. 2015; 1:149–157. [PubMed: 26181014]

12. Newman AM, Bratman SV, To J, Wynne JF, Eclov NC, Modlin LA, et al. An ultrasensitive method for quantitating circulating tumor DNA with broad patient coverage. Nat Med. 2014; 20:548–554. [PubMed: 24705333]

13. Siravegna G, Mussolin B, Buscarino M, Corti G, Cassingena A, Crisafulli G, et al. Clonal evolution and resistance to EGFR blockade in the blood of colorectal cancer patients. Nat Med. 2015; 21:795–801. [PubMed: 26030179]

14. Thress KS, Paweletz CP, Felip E, Cho BC, Stetson D, Dougherty B, et al. Acquired EGFR C797S mutation mediates resistance to AZD9291 in non-small cell lung cancer harboring EGFR T790M. Nat Med. 2015; 21:560–562. [PubMed: 25939061]

15. Hyman DM, Diamond EL, Vibat CR, Hassaine L, Poole JC, Patel M, et al. Prospective blinded study of BRAFV600E mutation detection in cell-free DNA of patients with systemic histiocytic disorders. Cancer Discov. 2015; 5:64–71. [PubMed: 25324352]

16. Melkonyan HS, Feaver WJ, Meyer E, Scheinker V, Shekhtman EM, Xin Z, et al. Transrenal nucleic acids: from proof of principle to clinical tests. Ann N Y Acad Sci. 2008; 1137:73–81. [PubMed: 18837928]

17. Su YH, Wang M, Brenner DE, Ng A, Melkonyan H, Umansky S, et al. Human urine contains small, 150 to 250 nucleotide-sized, soluble DNA derived from the circulation and may be useful in the detection of colorectal cancer. J Mol Diagn. 2004; 6:101–107. [PubMed: 15096565]

18. Reckamp KL, Melnikova VO, Karlovich C, Sequist LV, Camidge DR, Wakelee H, et al. A Highly Sensitive and Quantitative Test Platform for Detection of NSCLC EGFR mutations in Urine and Plasma. J Thorac Oncol. 2016; 10:1690–700.

19. Janne PA, Yang JC, Kim DW, Planchard D, Ohe Y, Ramalingam SS, et al. AZD9291 in EGFR inhibitor-resistant non-small-cell lung cancer. N Engl J Med. 2015; 372:1689–1699. [PubMed: 25923549]

20. Sequist LV, Soria JC, Goldman JW, Wakelee HA, Gadgeel SM, Varga A, et al. Rociletinib in EGFR-mutated non-small-cell lung cancer. N Engl J Med. 2015; 372:1700–1709. [PubMed: 25923550]

21. Wang S, Cang S, Liu D. Third-generation inhibitors targeting EGFR T790M mutation in advanced non-small cell lung cancer. J Hematol Oncol. 2016; 9:34. [PubMed: 27071706]

22. Goss G, Tsai CM, Shepherd FA, Bazhenova L, Lee JS, Chang GC, et al. Osimertinib for pretreated EGFR Thr790Met-positive advanced non-small-cell lung cancer (AURA2): a multicentre, open-label, single-arm, phase 2 study. Lancet Oncol. 2016; 12:1643–1652.

23. Khozin S, Weinstock C, Blumenthal GM, Cheng J, He K, Zhuang L, et al. Osimertinib for the Treatment of Metastatic Epidermal Growth Factor T970M Positive Non-Small Cell Lung Cancer. Clin Cancer Res. 2016

24. Mok TS, Wu YL, Ahn MJ, Garassino MC, Kim HR, Ramalingam SS, et al. Osimertinib or Platinum-Pemetrexed in EGFR T790M-Positive Lung Cancer. N Engl J Med. 2017; 376:629–640. [PubMed: 27959700]

25. Cross DA, Ashton SE, Ghiorghiu S, Eberlein C, Nebhan CA, Spitzler PJ, et al. AZD9291, an irreversible EGFR TKI, overcomes T790M-mediated resistance to EGFR inhibitors in lung cancer. Cancer Discov. 2014; 4:1046–1061. [PubMed: 24893891]

26. Walter AO, Sjin RT, Haringsma HJ, Ohashi K, Sun J, Lee K, et al. Discovery of a mutant-selective covalent inhibitor of EGFR that overcomes T790M-mediated resistance in NSCLC. Cancer Discov. 2013; 3:1404–1415. [PubMed: 24065731]

27. Jia Y, Juarez J, Li J, Manuia M, Niederst MJ, Tompkins C, et al. EGF816 Exerts Anticancer Effects in Non-Small Cell Lung Cancer by Irreversibly and Selectively Targeting Primary and Acquired Activating Mutations in the EGF Receptor. Cancer Res. 2016; 76:1591–602. [PubMed: 26825170]

28. Hata A, Niederst MJ, Archibald HL, Gomez-Caraballo M, Siddiqui FM, Mulvey HE, et al. Tumor cells can follow distinct evolutionary paths to become resistant to epidermal growth factor receptor inhibition. Nat Med. 2016; 3:262–9.

29. Marchetti A, Palma JF, Felicioni L, De Pas TM, Chiari R, Del Grammastro M, et al. Early Prediction of Response to Tyrosine Kinase Inhibitors by Quantification of EGFR Mutations in Plasma of NSCLC Patients. J Thorac Oncol. 2015; 10:1437–1443. [PubMed: 26295376]

30. Dawson SJ, Tsui DW, Murtaza M, Biggs H, Rueda OM, Chin SF, et al. Analysis of circulating tumor DNA to monitor metastatic breast cancer. N Engl J Med. 2013; 368:1199–1209. [PubMed: 23484797]

Abbreviations

ctDNA	circulating tumor DNA
EGFR	epidermal growth factor
NSCLC	non-small cell lung cancer
TKI	tyrosine kinase inhibitor
WT	wild type

|	
ddPCR	Droplet Digital PCR
NGS	next generation sequencing
LLoD	Lower Level of Detection
LLoB	Lower Limit of Blank
GEq	Genome Equivalents
CV%	Coefficient of Variation Percent

Significance

The modeling of tumor lysis through the day-to-day kinetics of ctDNA released into the blood and then into the urine is demonstrated in this proof of concept study in lung cancer patients receiving anti-EGFR tyrosine kinase inhibitors. This strategy may determine the specific clonal populations of cells which undergo apoptosis within the first week of therapy. This has important implications for developing combinational strategies to address inter- and intra-lesional heterogeneity and characterizing residual disease after initial drug exposure.
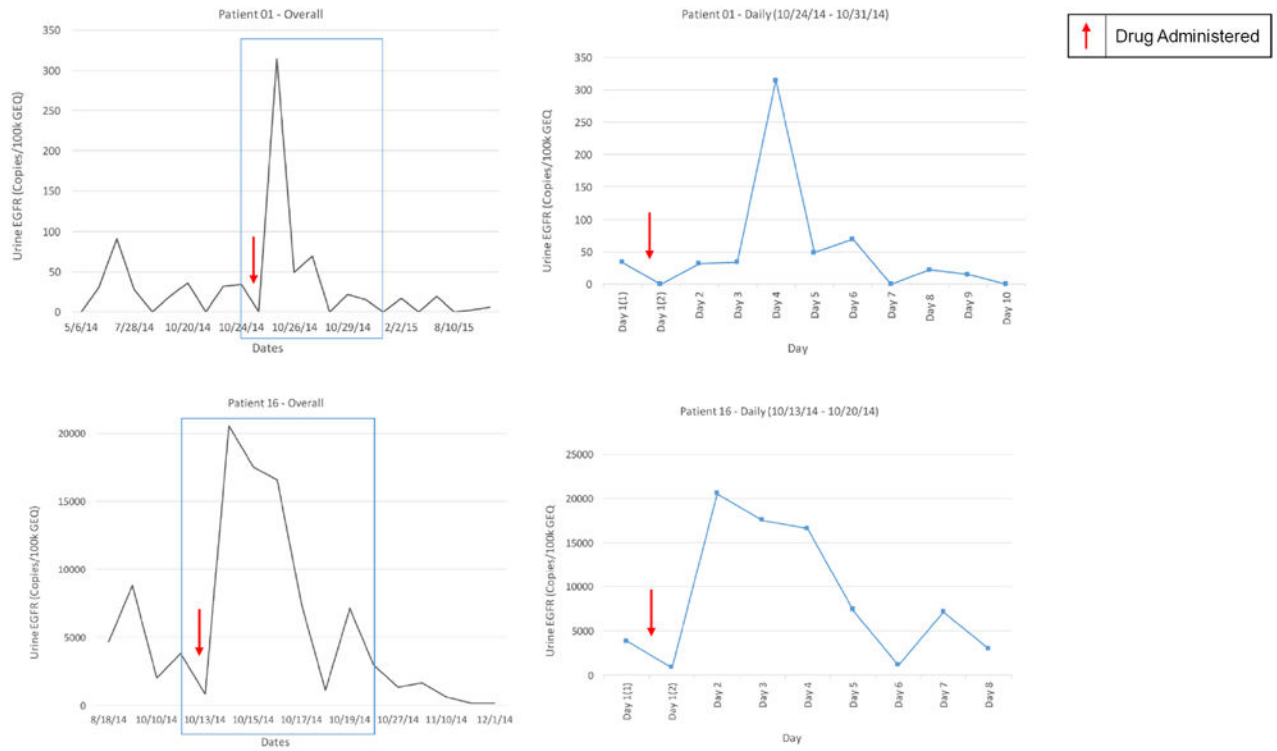
Figure 1. Dynamic changes in urinary ctDNA with time-points preceding osimertinib drug administration, time points immediately post administration, and several time-points later in therapy

Subjects 1 and 16. Data points of ctDNA copies suggest a significant change from baseline after osimertinib drug administration, and this is represented as a spike during the first week of therapy.
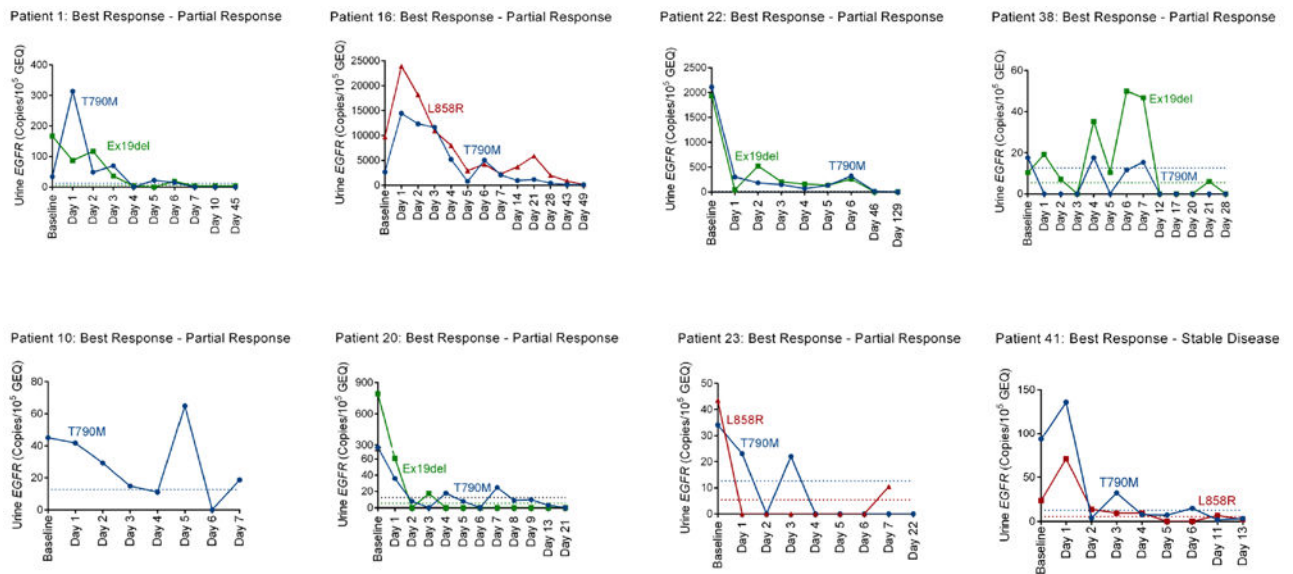
Figure 2. Daily dynamics of ctDNA EGFR mutation levels on second line osimertinib
Urine samples were collected from patients prior to osimertinib treatment as baseline and daily on treatment. A consistent pattern was observed with spikes during the first week followed by an overall decrease in the numbers of copies by day 7. Data points are mutant EGFR copies per 100,000 genome equivalents detected. Dashed lines indicate clinical detection cut-offs for the EGFR activating mutations (L858R = red, exon 19 deletions = green) and T790M (blue).
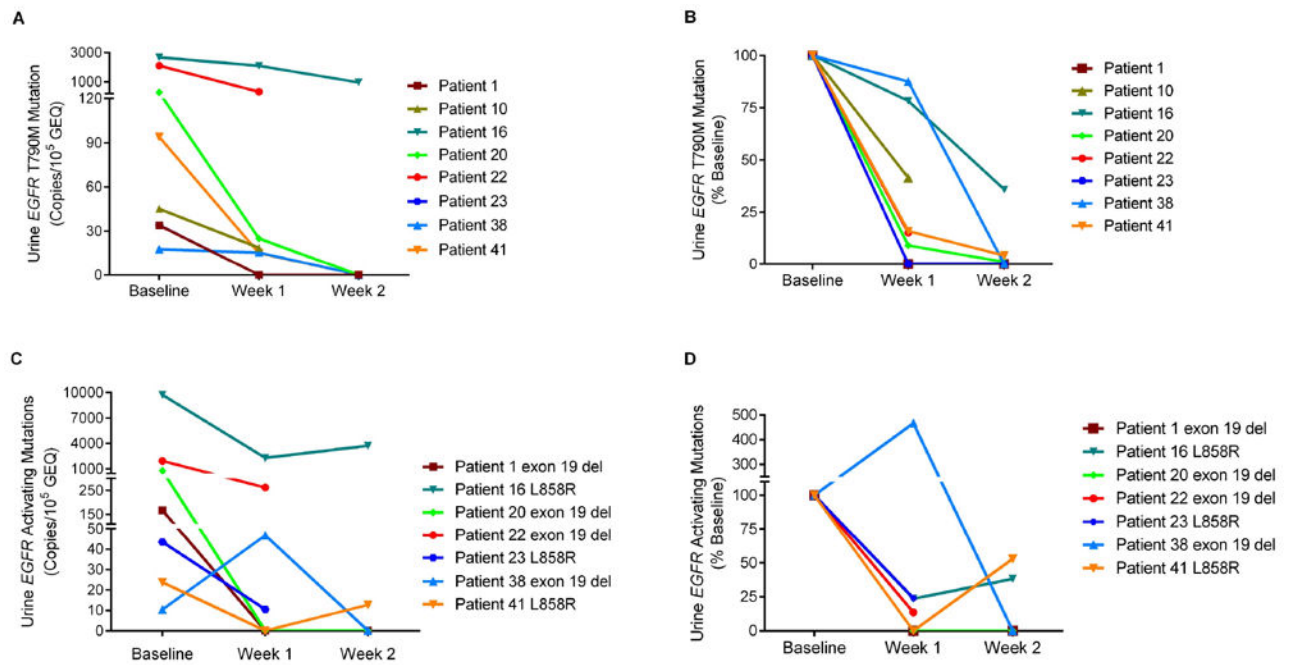
Figure 3. Quantification of *EGFR* mutation levels in urine of patients with NSCLC before and after 1 and 2 weeks of osimertinib

Urine samples were collected from patients prior to osimertinib and at week 1 or week 2 time points on treatment. T790M ctDNA and corresponding EGFR L858R or exon 19 deletion levels are shown as copies per 100,000 genome equivalents (1A, B) or as percent of respective baselines (1C, D). A significant relative decrease in T790M mutation signal from baseline was observed at week 1 and 2 on treatment (one-sided p-values of 0.014 and 0.045, respectively, using Wilcoxon's Test) (1C). Similar patterns were observed for the activating mutations L858R, exon 19 deletions at week 1 and week 2.
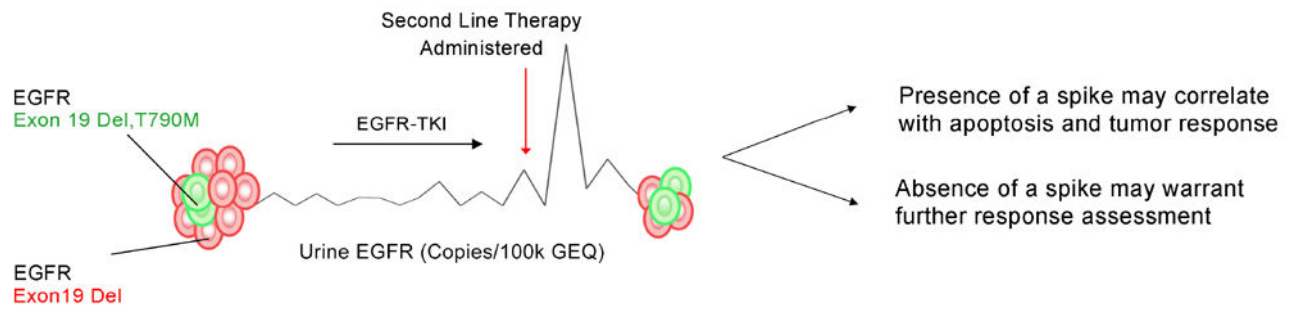
Figure 4. Potential applications of early response monitoring in *EGFR*-mutant NSCLC
Strategies that evaluate the daily kinetic changes in ctDNA during the first week of therapy will be explored to characterize response assessments based on the size, presence, or absence of peaks in ctDNA. A larger prospective analysis is underway to verify this in a larger cohort of patients with variable responses.

Table 1

Analytic performance of the urine ctDNA EGFR exon 19del, L858R, and T790M assays

For the T790M assay, a DNA blend with 160 mutant copies in a background of 18,181 WT GEq (0.011%) was prepared and distributed over 80 wells. For the exon 19 deletions and L858R assays, a DNA blend with 80 mutant copies in a background of 18,181 WT GEq (0.006%) was prepared and distributed over 80 wells. Following mutation enrichment NGS, the observed frequency distribution for counts of zero, one, two, and three copies across 80 replicates was compared to theoretical Poisson expectations (95% confidence intervals).

EGFR T790M[1] (LLoD = 2 copies, 0.011%)

Number of Mutant Copies	0-1		2	3
Expected (95% CI) for 160 copies/80 wells	32 (21-46)		22 (14-34)	14 (7-25)
Observed	22		22	18

EGFR exon 19 deletions[2] (LLoD = 1 copy, 0.006%)

Number of Mutant Copies	0	1	2	3
Expected (95% CI) for 80 copies/80 wells	29 (19-42)	29 (19-43)	15 (8-25)	5 (1-12)
Observed	34	20	9	2

EGFR L858R[2] (LLoD = 1 copy, 0.006%)

Number of Mutant Copies	0	1	2	3
Expected (95% CI) for 80 copies/80 wells	29 (19-42)	29 (19-43)	15 (8-25)	5 (1-12)
Observed	29	23	15	8

Table 2

Patient demographics - Detection of mutant *EGFR* in urine of patients with NSCLC who had relapsed on first-line anti-EGFR therapy.

Subject Number	Age (Yrs)	NSCLC[1] Tissue Mutation	Stage	# of *EGFR* T790M molecules per 10^5 GEq[2]	# of *EGFR*-activating mutation (L858R and/or exon 19 del) molecules per 10^5 Geq[2]	Second line anti-3rd gen EGFR TKI	Best Response on 1st / 2nd scan after second line therapy (RECIST)[5]	Time to progression on 3rd gen EGFR TKI (days)
1	68	T790M, exon 19 del	M1b	34	167	Osimertinib	48% reduction	210
10	59	T790M, L861Q	M1b	45	N/A[3]	Osimertinib	44% reduction	462
16	54	T790M, L858R	M1b	2684	9745	Osimertinib	75% reduction	118
20	57	T790M, exon 19 del	M1b	276	793	Osimertinib	53% reduction	N/A[6]
22	61	T790M, exon 19 del	M1b	2111	1932	Osimertinib	65% reduction	541
23	55	T790M, exon 19 del, L858R	M1b	34	43	Osimertinib	56% reduction	200
38	56	T790M, exon 19 del	M1a	18	10	Osimertinib	31% reduction	372
39	57	T790M, exon 19 del	M1a	< LloD[4]	<LloD[4]	Osimertinib	35% reduction	253
41	75	T790M, L858R	M1b	94	24	Osimertinib	9% reduction	246

Abbreviations:

[1] NSCLC = non-small cell lung cancer;

[2] EGFR = epidermal growth factor receptor; GEq, genome equivalents;

[3] N/A (EGFR activating mutation copies) = L861Q mutation was not tested;

[4] LLoD = number of mutant molecules below Lower Limit of Detection;

[5] RECIST = Response Evaluation Criteria in Solid Tumors v1.1;

[6] N/A (Time to Progression) = not yet reached.